Automatic two-stage IR and MMW image registration algorithm for concealed weapons detection

H.-M.Chen and P.K.Varshney

Abstract: A two-stage registration scheme for the concealed weapons detection (CWD) problem is developed. The goal is to automatically register images taken simultaneously from two different (infrared (IR) and millimetre wave (MMW)) but parallel sensors whose lines of sight (LOS) are close to each other. The purpose of the first stage is to register the images coarsely. A feature-based image registration algorithm based on human body silhouettes is developed at this stage. The pose parameters found at this stage are used as the starting search point for the second stage of the registration algorithm. At the second stage, maximisation of the mutual information measure between IR and MMW images is performed to improve the pose parameters obtained at the first stage. Two-dimensional partial volume interpolation is employed to estimate the joint histogram that is needed to calculate mutual information. The simplex search algorithm is utilised to maximise the MI measure. In both stages, the distortion between the two images is assumed to be a rigid body transformation. Experimental results indicate that the automated two-stage registration algorithm performs fairly well.

1 Introduction

Over the years, global terrorism and crime have grown. One key step in preventing terrorism and crime is to determine whether or not people are carrying weapons concealed underneath their clothing. Concealed weapons detection (CWD) is, therefore, an increasingly important problem [1]. It is a technological challenge that requires innovative solutions. A number of sensors based on different phenomenology are being developed to observe objects underneath people's clothing [2]. Each sensor has its limitations. For example, infrared (IR) imagers cannot penetrate heavy clothing and millimetre wave (MMW) images have poor resolution. In order to overcome these limitations, multiple sensors that provide complementary information may be employed for CWD [3]. Recently, IR and MMW sensors have been considered for CWD purposes since an IR sensor provides a high-resolution image, while a MMW sensor can penetrate through clothing. By fusing this complementary information, more complete information is anticipated, which could then be utilised to detect concealed weapons [4–6]. Once images from different sensors are available, it is necessary to find the corresponding points in the images before employing a fusion algorithm. In the image fusion algorithms presented in [4–6] results were quite encouraging, but it was assumed that either registered images were available prior to fusion or images were registered manually. Thus, in order to process the images in real time, there is a need for automatic registration algorithms. The focus of this paper is on the development of such an automatic registration algorithm for CWD applications.

We consider the following multi-modality image registration problem. Two images are taken simultaneously from two different (IR and MMW) but parallel sensors, whose lines of sight (LOS) are close to each other. Fig. 1 shows a schematic of the setup under consideration. Different characteristics of IR and MMW images make the registration problem quite challenging. One typical IR and MMW image pair is shown in Fig. 2. Different characteristics of IR and MMW images can be clearly seen. The goal is to determine the transformation parameters (scale, rotation angle, x-displacement and y-displacement) between the IR and MMW images so that the two images correspond to each other after transforming one of the images.

Image registration is a fundamental task in image processing with applications in areas such as remote sensing [7], biomedical imaging [8], and computer vision [9]. Depending upon the chosen feature space, image registration methods can be divided into two categories: area-based and feature-based methods. An excellent survey of these techniques can be found in [10]. A newly developed area-based registration algorithm using mutual information as the similarity measure has been found to be very effective for many multi-modality image registration problems [11, 12]. In order to apply this MI-based registration technique successfully, initial misregistration must be small enough that it is within the capture range of the subsequent optimisation scheme [13]. Otherwise, the maximum found is very likely to be just a local maximum. Because of this, we propose a two-stage registration strategy: coarse registration followed by fine registration. The goal of the first stage is to register the IR and MMW

IEE Proceedings online no. 20010459

DOI: 10.1049/ip-vis:20010459

Paper received 23rd January 2001

The authors are with the Department of Electrical Engineering and Computer Science, 121 Link Hall, Syracuse University, Syracuse, NY 13244, USA

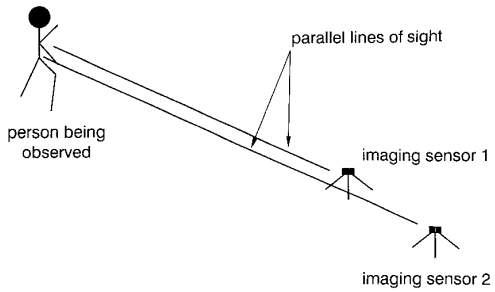

Fig. 1 *Set-up considered in our application*

images coarsely, so that the result obtained can be used as the initial starting point of the search algorithm used in the second stage for the maximisation of the mutual information of IR and MMW images.

For the first stage, a feature-based registration algorithm is developed. The features that we employ are the body silhouettes in both IR and MMW images. Two image thresholding algorithms are developed to obtain the body silhouettes from each image. Binary correlation is then used to register the two extracted body silhouettes. A mask construction algorithm is also developed. The purpose of this mask is to select the right peak in the 2-D correlation function. At this stage, we assume the transformation needed is only a rigid body transformation without rotation. Furthermore, we assume that the scale factor can be calculated based on the sensor parameters such as the field of view, focal length, and the distances between the person being observed by the two imagers. Therefore, the transformation parameters that need to be determined at the first stage are the x-displacement and y-displacement only. The rotation angle and scale factor are determined more accurately during the second stage.

In the second stage of our algorithm, maximisation of mutual information for registration is carried out. We use

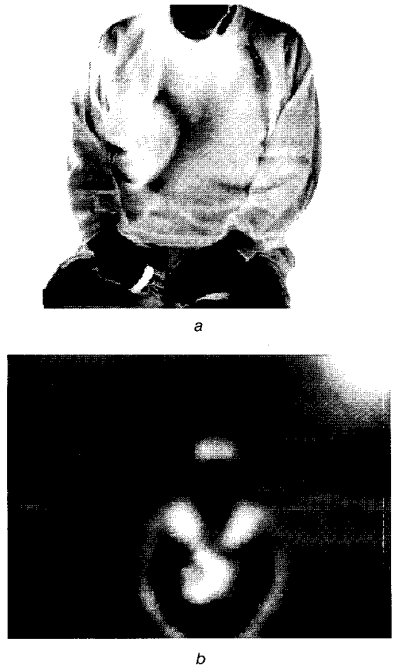

a

b

Fig. 2 *One typical outdoor IR and MMW image pair taken simultaneously from parallel sensors*

a IR image
b MMW image

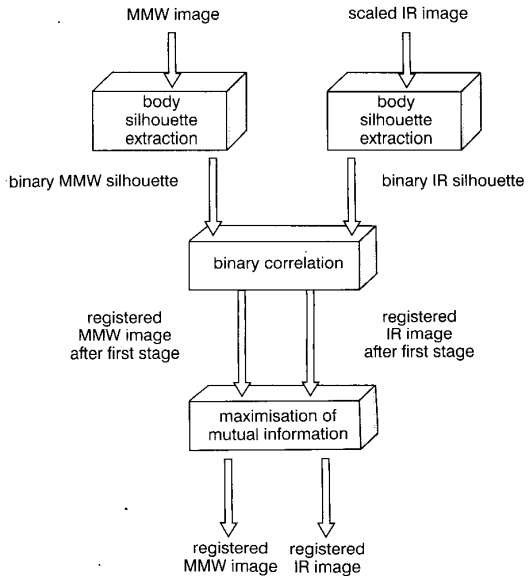

Fig. 3 *Overview of the two-stage registration algorithm*

the 2-D implementation of the partial volume interpolation (PV) method [12] to estimate the joint probability distribution that is needed to compute the mutual information metric. The simplex method [14] is employed to search for the maximum because of its simpler implementation. An overview of our two-stage registration algorithm is provided in Fig. 3.

2 Algorithm

The algorithm developed for the first stage is based on the following characteristics of available IR and MMW images for the CWD application:

(i) The body is darker than the background in IR images.
(ii) Except for the transition part in MMW images, the body is either darker or brighter than the background.
(iii) The background is smoother than the body in MMW images.

The first two characteristics can be easily seen from Fig. 2. In order to visualise the third characteristic, we define a smoothness measure SM corresponding to a pixel in an image as the second moment about its mean within its 3×3 neighborhood, i.e.

$$SM(X, Y) = \sum_{dx=-1}^{1} \sum_{dy=-1}^{1} (I(x + dx, y + dy) - m(x, y))^2/9 \quad (1)$$

where $I(x, y)$ is the grey level intensity of the pixel (x, y), and $m(x, y)$ is the mean within the 3×3 neighbourhood of the current pixel (x, y). The smoothness measure $SM(x, y)$ of the MMW image shown in Fig. 2 is displayed as an image in Fig. 4. From Fig. 4, we can easily see that the background is much smoother than the body in MMW images because most of the background is darker than the body.

The complete block diagram of our registration algorithm at the first stage is shown in Fig. 5. The transformation parameters that need to be found at this stage are the x-displacement and y-displacement. It is assumed that the scale factor can be obtained from the sensor parameters

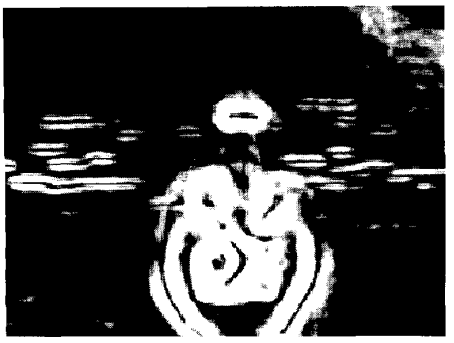

Fig. 4 *Smoothness measure for the MMW image shown in Fig. 2*

and the distances between sensors to the person being observed. Here, we calculate the scale factor S using the following expression:

$$S = S_0 \times \frac{d_{IR}}{d_{MMW}} \tag{2}$$

where d_{IR} and d_{MMW} are the distances from the person being observed to the IR sensor and the MMW sensor, respectively. S_0 is the scale factor when the two sensors are co-located, that is $d_{IR} = d_{MMW}$. In our experiments, S_0 equals 0.3125, which is determined by manually registering one pair of images taken from equal distance. The main tasks involved in the algorithm shown in Fig. 5 include two body silhouette extraction algorithms, a mask construction algorithm and a binary correlation algorithm. The details of these tasks are given below.

2.1 Body silhouette extraction from IR images

The human body temperature is generally higher than the temperature of the background. Therefore, in IR images the body portion is darker than the background. This characteristic of IR images suggests that we can use a histogram-based thresholding operation to separate the body from the background. Based on the available IR images, we found that the desired threshold corresponds to one of the local minima of the histogram. Therefore, we determine the set of all local minima, which are all

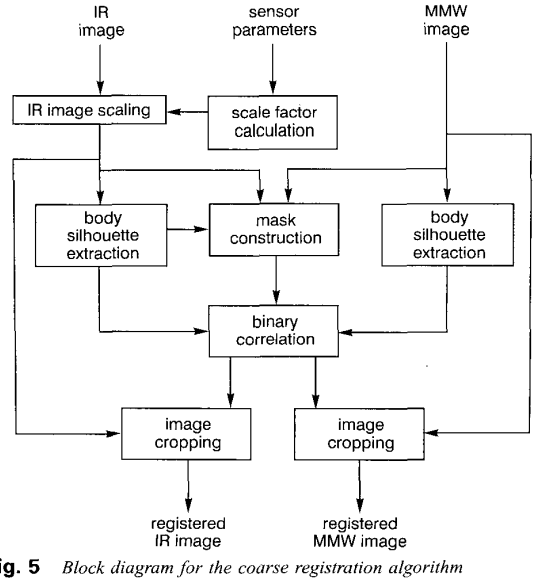

Fig. 5 *Block diagram for the coarse registration algorithm*

potential threshold candidates, and select a threshold from this set. The criterion we use to select the threshold to extract the body is 'matrix-shape connectivity', or *SC* [15], which is defined through the co-occurrence matrix [16], and is stated below.

Let $I(m, n)$, $0 < m < M+1$, $0 < n < N+1$, represent an $M \times N$ image containing l grey levels. The size of the corresponding co-occurrence matrix is $l \times l$. Its (i, j)th entry p_{ij} is the probability of the grey level pair (i, j) in the original image. It is defined as follows:

$$p_{ij} = t_{ij} \Big/ \left(\sum_{i=0}^{l-1} \sum_{j=0}^{l-1} t_{ij} \right) \tag{2}$$

where

$$t_{ij} = \sum_{m=i}^{M} \sum_{n=1}^{N} \delta(m, n) \tag{3}$$

and

$$\delta(m, n) = 1 \quad \text{if} \begin{cases} I(m, n) = i, I(m, n+1) = j \\ \text{and/or} \\ I(m, n) = i, I(m+1, n) = j \end{cases} \tag{4}$$

$$\delta(m, n) = 0 \quad \text{otherwise}$$

Let t be the grey level associated with the image threshold. It partitions the co-occurrence matrix into four distinct blocks. The block probabilities are defined as

$$B_1(t) = \sum_{i=0}^{t} \sum_{j=0}^{t} p_{ij} \tag{5a}$$

$$B_2(t) = \sum_{i=0}^{t} \sum_{j=t+1}^{l-1} p_{ij} \tag{5b}$$

$$B_3(t) = \sum_{i=t+1}^{l-1} \sum_{j=t+1}^{l-1} p_{ij} \tag{5c}$$

$$B_4(t) = \sum_{i=t+1}^{l-1} \sum_{j=0}^{t} p_{ij} \tag{5d}$$

The measure 'shape connectivity' (SC) is then defined as

$$SC(t) = \frac{Min(B_1(t), B_4(t))}{B_2(t) + B_3(t)} \tag{6}$$

We selected the desired threshold that gives the largest SC measure. The reason we choose this criterion is due to the fact that the desired threshold should result in an ideal binary image containing only two connected regions. One region corresponds to the body silhouette and the other corresponds to background. The SC measure proposed by Lie provides a quantitive method to measure the connectivity of the threshold image. Based on the set of available IR images we found that shape connectivity is very effective for our purpose.

Owing to its very nature, it is necessary to smooth the histogram before we can find the set of local minima. Here we use smoothing splines for this purpose [17, 18]. In this method, a parameter λ is used to obtain a compromise between the desire for an approximation that is reasonably close to the data and the requirement of a function that is sufficiently smooth. In our case, we iteratively applied this smoothing procedure for $\lambda = 1, 2, 3 \ldots$ until the resulting histogram contains M modes. The value of M equal to or greater than 3 was found to be adequate for our purpose.

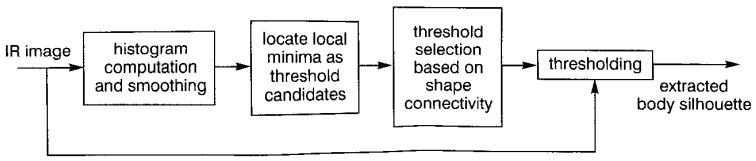

Fig. 6 *Body extraction algorithm for IR images*

The main steps of our body extraction algorithm for IR images are summarised in Fig. 6. An example illustrating the steps of the algorithm is given in Fig. 7. Note that the IR image is scaled prior to body extraction. Figs. 7*a* and *b* show the scaled IR image and its corresponding histogram. The smoothed histogram with $M=3$ along with threshold candidates is shown in Fig. 7*c*. Two thresholded images corresponding to the set of two potential threshold candidates are shown in Figs. 7*d* and *e*. The threshold value used and the shape connectivity of each thresholded image are also shown. Comparing the shape connectivity SC in Figs. 7*d* and *e*, we choose the one shown in Fig. 7*e* as the desired body silhouette.

2.2 Body silhouette extraction from MMW images

The algorithm developed to extract the body silhouette from MMW images is based on the characteristic of MMW images that except for the transition part in MMW images, the body is either darker or brighter than the background. By examining the available MMW images, it is observed that there is only one major mode in the histogram, and the histogram of the background falls within the main lobe of the histogram of the entire image. Therefore, if we can separate the image that corresponds to the main lobe of the histogram from the entire image, we can approximately extract the subject (body in our case) from the background. We have shown in [19] that an exact extraction of the body silhouette is not essential for producing a peak on the 2-D correlation function, since the extracted body silhouette preserves the boundary of the body quite well. It is because the light reflections always appear at the boundary of the observed person. Segmenting the part of the image that corresponds to the main lobe of the histogram requires the determination of two suitable thresholds. We use the same smoothing procedure as for IR images, with M equal to one. After smoothing the histogram, we locate the mode and the two points of inflection. They are denoted as P, f_1 and f_2 respectively. Then we determine the two thresholds t_1 and t_2 as follows:

$$t_1 = P - L_1 \cdot (P - f_1) \tag{7a}$$

$$t_2 = P + L_2 \cdot (f_2 - P) \tag{7b}$$

where L_1 and L_2 are two constants that need to be determined empirically. $L_1 = L_2 = 1.5$ was satisfactory for our application. Once we have found the two thresholds, we threshold the image with each threshold separately, invert one of the thresholded images, and then add them up to obtain the approximate silhouette of the body. Fig. 8 summarises the steps and an example is shown in Fig. 9. Fig. 9*a* and *b* show the original MMW image and its corresponding histogram. The smoothed histogram with $M=1$ along with points of inflection and thresholds is shown in Fig. 9*c*. The two thresholded images are shown in Figs. 9*d* and *e*. Fig. 9*f* is the composite of the two thresholded images and represents the approximate body silhouette determined by our algorithm.

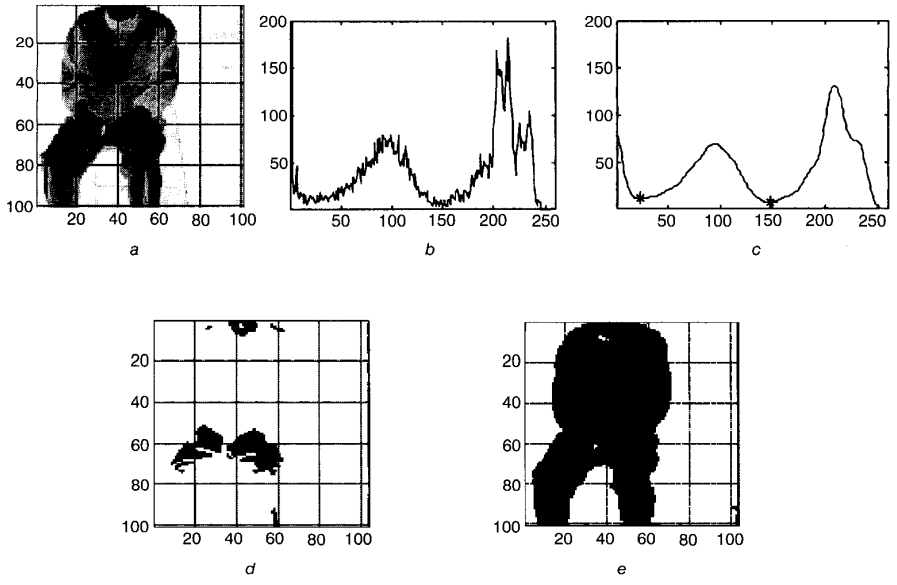

Fig. 7 *Example illustrating body silhouette extraction from IR images*

a Scaled IR image
b Corresponding histogram
c Smoothed histogram, $M=3$
d Thresholded image, $t=23$, $SC=2.3539$
e Thresholded image, $t=148$, $SC=16.5714$

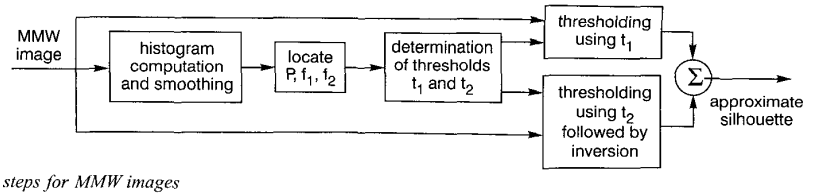

Fig. 8 *Body extraction steps for MMW images*

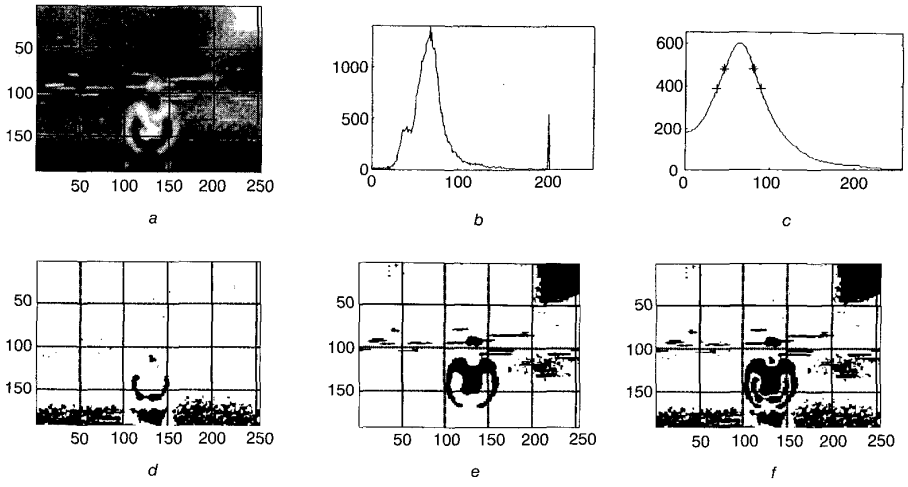

Fig. 9 *Example illustrating body silhouette extraction from MMW images*

a Original MMW image
b Corresponding histogram
c Smoothed histogram, $M = 1$
d Thresholded image
e Thresholded image
f Composite of thresholded images *d* and *e*

2.3 Binary correlation

The goal of this step is to determine the x- and y-displacements by correlating the extracted binary IR and MMW silhouette images. Usually, a binary image is represented by pixel values 0 and 1. This representation has one drawback for the correlation operation. While maximising the correlation function, we attempt to match only the parts represented by pixel value 1 in both images as much as possible and neglect the influence of the parts represented by pixel value 0 in both images. To overcome this drawback, we use 1 and -1 to represent the two levels of the thresholded images, so that by maximising the correlation function, both parts are matched as much as possible. In our algorithm, we implement the correlation operation in the frequency domain. By implementing the correlation in the frequency domain, the images were inherently made periodic and normalisation of the correlation is no longer necessary, since the area of the overlap is now fixed. In order to utilise the fast Fourier transform, we first pad both images with zeros so that both image sizes become 256×256. The result of correlating the extracted IR silhouette shown in Fig. 7*e* with the extracted MMW silhouette shown in Fig. 9*f* is shown in Fig. 10.

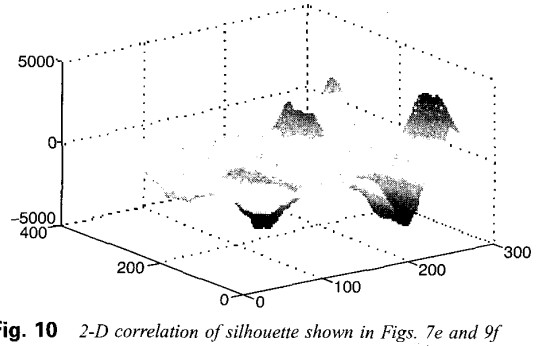

Fig. 10 *2-D correlation of silhouette shown in Figs. 7e and 9f*

Notice that the correlation value at the point (x, y) is equal to the correlation of binary IR and MMW silhouette images when the centre of the binary IR image corresponds to the point (x, y) in the MMW image. Also, there are multiple peaks, and the desired one may not be the highest one. They result from the imperfect silhouette extracted from the MMW image due to noise and unwanted light reflections. The method we used to overcome this problem is described next.

2.4 Mask construction

The thresholded MMW image contains a lot of noise that results in multiple peaks in the 2-D correlation function. Sometimes the strengths of the incorrect peaks are stronger than the strength of the correct one. Therefore, it is necessary to develop a procedure to identify the right peak that yields correct x- and y-displacements. We take advantage of the observation that the intensity of background of the MMW image is smoother than that of the body portion, as described at the beginning of Section 2. Using this property, we develop the following algorithm to construct a mask to select the right peak. First we define a binary map that indicates whether a pixel is smooth or not according to eqn. 1 as follows:

$$B(x,y) = \begin{cases} 0 & \text{if } SM(x,y) < t_b \\ 1 & \text{if } SM(x,y) \geq t_b \end{cases} \quad \text{for } 1 \leq x \leq m,\ 1 \leq y \leq n \tag{8}$$

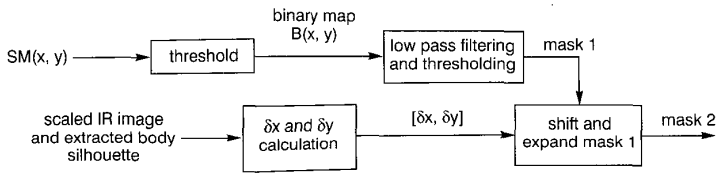

Fig. 11 *Block diagram for the mask construction algorithm*

where t_b is a fixed threshold. We found $t_b = 30$ to be satisfactory for our application. $SM(x, y)$ was defined by eqn. 1 and m, n specify the size of the MMW image. By passing the binary map defined above through a low pass filter and thresholding it, a binary mask M1 which can be used to locate the extracted MMW body silhouette is obtained. The threshold we used was half of the maximal value of the low pass filtered binary map. The mask that can be applied on the 2-D correlation function directly to select the right peak can be obtained by shifting the mask M1. We first shift M1 by the amount δx and δy along the x and y directions, respectively, and enlarge the resulting mask by zero padding it into size 256×256, which is the size of the 2-D correlation function. δx and δy are the distances along the x- and y-directions between the centre of the IR image and the centre of the extracted IR body silhouette image. Fig. 11 summarises the steps of the algorithm, and one example is given in Fig. 12. The original MMW image is the one shown in Fig. 9*a*. The binary map $B(x, y)$, original mask M1, and desired mask M2 are shown in Figs. 12*a–c*. The result of applying M2 to the 2-D correlation function shown in Fig. 10 is shown in Fig. 12*d*. Note that we can now select the maximum to determine the x- and y-displacements successfully.

2.5 Maximisation of mutual information

Once the IR and MMW images are registered coarsely, the MI-based registration techniques can be employed to improve the result. Some implementations of this technique are available in the literature. Wells *et al.* [11] randomly sampled a fixed number of pixels many times to estimate the joint histogram needed to compute the MI metric. A stochastic optimisation scheme is then used to maximise the mutual information. Maes *et al.* [12] proposed a method called partial volume interpolation (PV) to estimate the joint histogram and Powell's optimization algorithm [20] to maximise the MI metric. For our application, we use PV interpolation to estimate the joint histogram and the simplex method [14] to find the maximum of the mutual information measure because of its simplicity. The result obtained from the first stage is used as the starting point for search at this stage. Our experiments show that in this manner, the global maximum of the MI measure can always be found for our application.

3 Experimental results

Registration results for two IR and MMW image pairs are shown in this section. Figs. 13*a*, *b* and 14*a*, *b* are original IR and MMW images, and Figs. 13*c* and 14*c* and 13*d* and 14*d* are the registered MMW images at the first and second stage, respectively, with the boundary from the corresponding IR images superimposed. The distance information for each original image is indicated in the Figure captions. The pose parameters, scale, rotation angle, x- (vertical-) displacement and y- (horizontal-) displacement, found at each stage are indicated for the registered images. From Figs. 13 and 14, we can see the improved accuracy after the second stage of our algorithm because the scale factor and the rotation angle are also taken into account at the second stage.

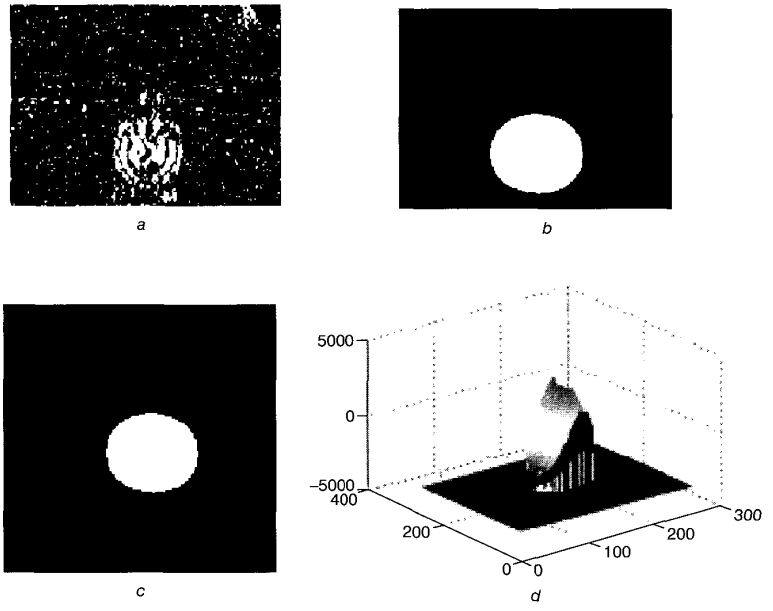

Fig. 12 *Example showing the mask construction steps*

a Binary map $B(x, y)$
b M1
c M2
d 2-D correlation function after applying M2

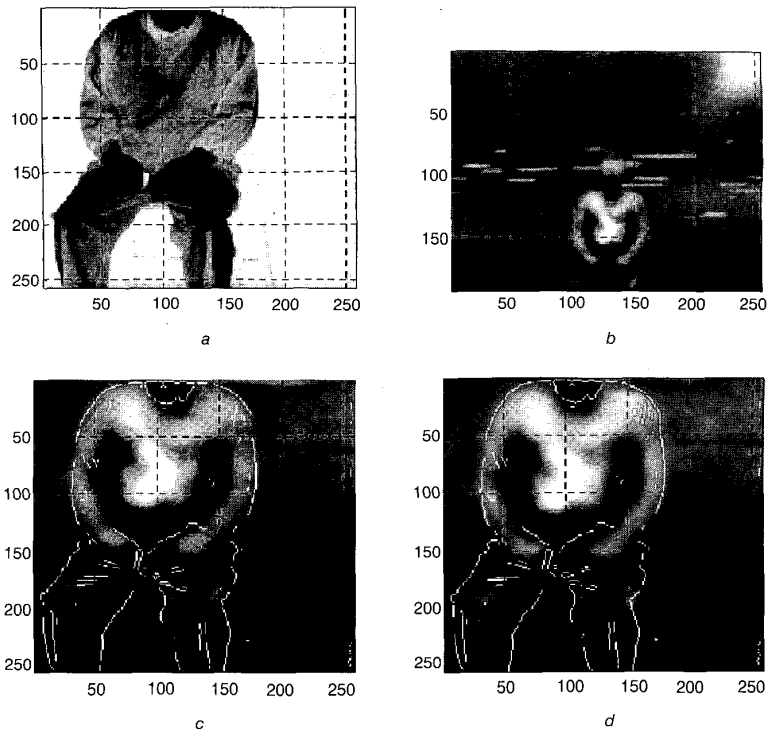

Fig. 13 *Result 1*

a Original IR image (19 feet)
b Original MMW image (15 feet)
c Registered MMW image at the first stage with the body edges from IR image superimposed (pose parameters: 0.40, 0, 62.5, 12.5)
d Registered MMW image at the second stage with the body edges from IR image superimposed (pose parameters: 0.41436, −3.1482, 64.1023, 14.2138)

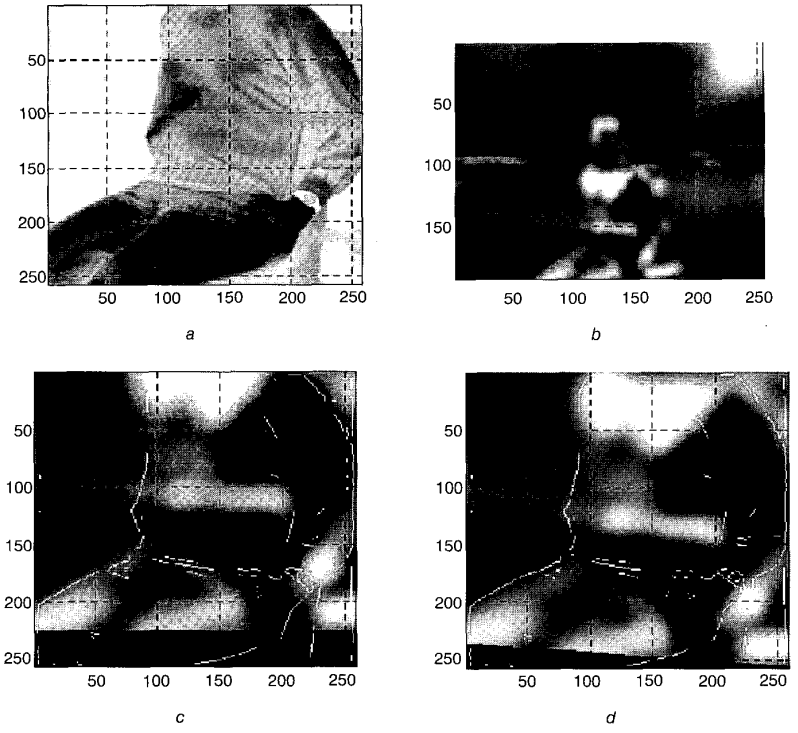

Fig. 14 *Result 2*

a Original IR image (14 feet)
b Original MMW image (12 feet)
c Registered MMW image at the first stage with the body edges from IR image superimposed (pose parameters: 0.36, 0, 61.5, −5.5)
d Registered MMW image at the second stage with the body edges from IR image superimposed (pose parameters: 0.36289, −4.5404, 53.8153, −6.2946)

4 Summary and conclusions

In this paper, we developed an automated image registration algorithm for CWD applications. A two-stage scheme is proposed to successfully employ the existing MI-based registration technique. The input data are the corresponding pair of IR and MMW images and the distances between the sensors and the person under observation. The requirements for our algorithm to perform satisfactorily are: (i) the line of sights of IR and MMW sensors are parallel and as close as possible to each other, such that a two-dimensional rigid body transformation can account for the misregistration between the two images; and (ii) the body silhouette of the person being investigated is visible in both IR and MMW images, because it is the body silhouette that is used as the common feature while developing the algorithm at the first stage of our method. At the second stage of our algorithm, we maximise the mutual information measure to refine the parameters found at the first stage. Our experiments show that when the requirements mentioned above are satisfied, excellent results can be obtained. The algorithm needs to be extended when the conditions are not satisfied or when other sensing methods are employed.

5 Acknowledgments

We would like to thank Mark Alford, Dave Ferris, Liane Ramac, Adel Slamani, and Mucahit Uner for their help and encouragement during the course of this work. The data used in this work was provided by the Air Force Research Laboratory, Rome Research Site, and the National Institute of Justice. This effort was supported by the Air Force Research Laboratory, Air Force Materiel Command, USAF, under grant number F30602-95-1-0027, and the Defense Advanced Research Project Agency under grant no. N66001-99-1-8922.

6 References

1 CURRIE, N.C., DEMMA, F.J., FERRIS, D.D., Jr., McMILLAN, R.W., and WICKS, M.C.: 'ARPA/NIJ/Rome Laboratory concealed weapon detection program: An overview', *Proc. SPIE-Int. Soc. Opt. Eng.*, 1996, **2755**, pp. 492–502

2 CURRIE, N.C., DEMMA, F.J., FERRIS, D.D. Jr., KWASOWSKY, B.R., McMILLAN, R.W., and WICKS, M.C.: 'Infrared and millimetre wave sensors for military special operations and law enforcement applications', *Int. J. Infrared Millim. Waves*, 1996, **17**, (7), pp. 1117–1138

3 CURRIE, N.C., DEMMA, F.J., FERRIS, D.D., Jr., McMILLAN, R.W., WICKS, M.C., and ZYGA, K.: 'Image sensor fusion for concealed weapon detection', *Proc. SPIE-Int. Soc. Opt. Eng.*, 1997, **2942**, pp. 71–81

4 UNER, M.K., RAMAC, L.C., VARSHNEY, P.K., and ALFORD, M.: 'Concealed weapon detection: An image fusion approach', *Proc. SPIE-Int. Soc. Opt. Eng.*, 1997, **2942**, pp. 123–132

5 RAMAC, L.C., UNER, M.K., VARSHNEY, P.K., ALFORD, M., and FERRIS, D.: 'Morphological filters and wavelet-based image fusion for concealed weapons detection', *Proc. SPIE-Int. Soc. Opt. Eng.*, 1998, **3376**, pp. 110–119

6 ZHANG, Z., and BLUM, R.S.: 'Region-based image fusion scheme for concealed weapon detection'. Proceedings of 30th CISS conference, Baltimore, MD, 1997

7 THOMAS, I.L., BENNING, V.M., and CHING, N.P.: 'Classification of remotely sensed images' (Adam Hilger, Bristol, England, 1986)

8 STYTZ, M.R., FRIEDER, G., and FRIEDER, O.: 'Three-dimensional medical imaging: Algorithms and computer systems', *ACM Comput. Surv.*, 1991, **23**, (4), pp. 421–424

9 KATURI, R., and JAIN, R.C.: 'Computer vision: Principles' (IEEE Computer Society Press, Los Alamitos, CA, 1991)

10 BROWN, L.G.: 'A survey of image registration techniques', *ACM Comput. Surv.*, 1992, **24**, (4), pp. 325–376

11 WELLS, W., VIOLA, P., ATSUMI, H., NAKAJIMA, S., and KIKINIS, R.: 'Multi-modal volume registration by maximisation of mutual information', *Med. Image. Anal.*, 1996, **1**, (1), pp. 35–51

12 MAES, F., COLLIGNON, A., VANDERMEULEN, D., MARCHAL, G., and SUETENS, P.: 'Multimodality image registration by maximisation of mutual information', *IEEE Trans. Med. Imaging*, 1997, **16**, (2), pp. 187–198

13 STUDHOLME, C., HILL, D.L.G., and HAWKES, D.J.: 'Automated three-dimensional registration of magnetic resonance and positron emission tomography brain images by multiresolution optimization of voxel similarity measures', *Med. Phys.*, 1997, **24**, (1), pp. 25–35

14 NELDER, J.A., and MEAD, R.: 'A simplex method for function minimization', *Comput. J.*, 1965, **7**, (4), pp. 308–313

15 LIE, W.: 'Automatic target segmentation by locally adaptive image thresholding', *IEEE Trans. Image Process.*, 1995, **4**, (7), pp. 1036–1041

16 CHANDA, B., and MAJUMDER, D.D.: 'A note on the use of the gray-level co-occurrence matrix in threshold selection', *Signal Process.*, 1988, **15**, (2), pp. 149–167

17 UNSER, M., ALDROUBI, A., and EDEN, M.: 'B-spline signal processing: Part I—theory', *IEEE Trans. Signal Process.*, 1993, **41**, (2), pp. 821–833

18 UNSER, M., ALDROUBI, A., and EDEN, M.: 'B-spline signal processing: Part II—efficient design and applications', *IEEE Trans. Signal Process.*, 1993, **41**, (2), pp. 834–848

19 CHEN, H.: 'Registration of IR and MMW images for concealed weapons detection'. Master's thesis, Department of Electrical Engineering and Computer Science, Syracuse University, 2000

20 POWELL, M.: 'An efficient method of finding the minimum of a function of several variables without calculating derivatives', *Comput. J.*, 1964, **7**, pp. 155–163